On-chip actuation for waveguide alignment

Tichem, Marcel; Peters, Tjitte-Jelte; Wu, Kai

Publication date
2018

Document Version
Final published version

Published in
Mikroniek: vakblad voor precisie-technologie

ON-CHIP ACTUATION FOR WAVEGUIDE ALIGNMENT

Recent decades have seen impressive developments in the field of integrated photonics. Chips with complex photonic functionality can presently be designed and fabricated. Photonic packages consist of one or more PICs, as well as other (micro-optical) components, and a fibre (array) to establish the external optical interface. A core challenge is the assembly and packaging of these complex devices, involving sub-µm alignment of components. To overcome the limitations in multi-chip photonic packaging, a concept is proposed which uses on-chip actuators for the fine-alignment of flexible waveguide structures.

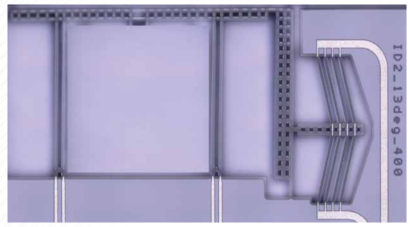

MARCEL TICHEM, TJITTE-JELTE PETERS AND KAI WU

Motivation

Chips with photonic functions, i.e. photonic integrated circuits (PICs), with complex functionality can presently be designed and fabricated at cost levels which are acceptable for a variety of applications [1]. Photonic packages consist of one or more PICs, as well as other (micro-optical) components, and a fibre (array) to establish the external optical interface. A core challenge is the assembly and packaging of these complex devices.

Assembly and packaging in the photonic domain is much less standardised compared to the microelectronic domain, and is a dominant cost factor. Particularly, the precise, sub-µm alignment of components is demanding. The currently dominant industrial approach to assembly is to use micro-positioners in a semi-automatic process for handling of components and joining methods like adhesive joining for locking in the final position.

Here, the aim is to reduce cost as well as assembly time by proposing a new concept, which exploits MEMS technology for the fine-alignment of flexible optical waveguide structures [2] [3] [4]. The concept has the potential to allow for full automation of the assembly process, thus reducing operator involvement. It is developed for new generations of photonic packages, containing multiple PICs with multiple optical I/O.

Figure 1 shows a schematic package overview, which combines an InP (indium phosphide) PIC with active optical functions (e.g., lasers and detectors) and a TriPleX-based PIC (Si_3N_4 waveguide cores in SiO_2 cladding material [5]) with passive optical functions. The TriPleX PIC acts as an interposer chip, to interface the InP PIC on one end to an optical fibre array at the other end. Its main functions are spot size conversion and waveguide pitch conversion. To prevent losses when interfacing waveguides, the spot sizes should match. The spot size at the InP interface is ~3 µm, whereas on the fibre interface the spot size is ~8 µm. One of the advantages of the TriPleX technology is that it allows on-chip spot size conversion.

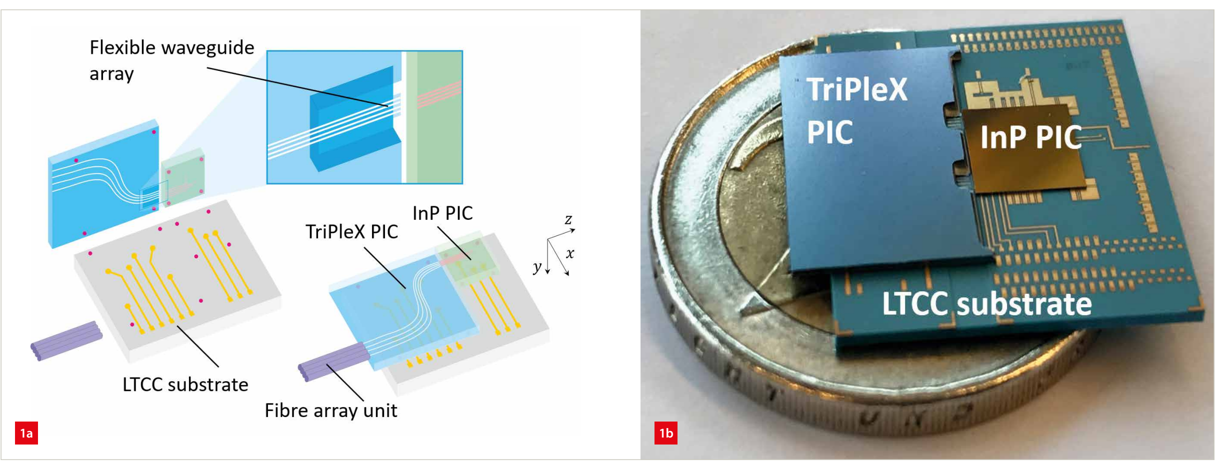

1 *Multi-chip photonic package.*
(a) Schematic overview.
(b) Flip-chip bonded InP and TriPleX PIC on a common substrate (LTCC, Low Temperature Co-fired Ceramics). (Courtesy of PHASTFlex consortium [4])

AUTHORS' NOTE

Associate professor Marcel Tichem and Ph.D. candidates Tjitte-Jelte Peters and Kai Wu are all attached to the Micro and Nano Engineering research group in the Department of Precision and Microsystems Engineering at Delft University of Technology, the Netherlands.

m.tichem@tudelft.nl
www.pme.tudelft.nl

The next sections introduce the alignment concept, present a typical design, and describe results.

Alignment concept

The assembly process is split into two steps: chip pre-assembly and waveguide fine-alignment. Chip pre-assembly is done by flip-chip placement and bonding of the two PICs on a common carrier. The waveguide positions are well-defined with respect to the active surface of the PIC, hence flip-chip bonding allows obtaining good precision in initial alignment.

When using small solder bumps, the initial precision can be controlled within ~1-2 µm. This is sufficient for the less critical alignment directions (translation in the *z*-direction, rotation in the *x*- and *y*-direction, see Figure 1). The remaining error in the critical directions (translation in *x*- and *y*-direction, rotation in *z*-direction) is subsequently compensated by a fine-alignment step, using flexible waveguide beams and MEMS (microelectromechanical system)-based functions, which are integrated with the TriPleX PIC.

Three main functions are needed on the TriPleX chip for waveguide fine-alignment: (1) flexible waveguide structures, (2) actuators for positioning the waveguide structures, and (3) a locking function to maintain the final position. Here, the focus is on flexible waveguides and positioning; the locking function is topic of further investigation.
The functions are realised by post-processing of a TriPleX wafer. The optimal position is found in an active alignment scheme, i.e. by measuring and maximising the coupled power while moving the waveguide beams. To this end, light sources, detectors, and alignment waveguides are added to the InP and TriPleX PIC design. The targeted precision, waveguide-to-waveguide, is 100 nm. Given the precision of the chip pre-assembly process, the required motion range (translation directions) for the waveguide beams is in the order of 4 µm.

Design

The MEMS functions are fabricated in the optical stack of the TriPleX material platform, which is a 16 µm-thick silicon dioxide/silicon nitride (SiO_2/Si_3N_4) layer on top of a silicon wafer. This is an innovation in itself, as the usual building material for MEMS is silicon. A challenge in the fabrication of SiO_2-based MEMS is the presence of significant compressive stress, due to the growth of the layer at high temperature (~1,000 °C). The stress easily leads to fracturing of the structures when released from the wafer.
A release process was developed to achieve reliable fabrication of the structures [6]. In this process, when the waveguide and actuator structures are defined by patterning the SiO_2 stack, deep trenches are etched into the Si wafer. Subsequently, the structures are released by etching the Si, starting at the bottom of the Si trench. The initially significant Si layer underneath the SiO_2 structures prevents their fracturing.
A typical design consists of an array of waveguide beams, see Figure 2. The beams have a typical cross-section of ~16x20 µm^2, and a length of up to ~1,000 µm. The waveguide beams are connected at their free ends with a cross-bar. In this way, the lithographically defined waveguide pitch is preserved, and the number of actuators required for positioning is limited.

Thermal actuators are used for positioning the waveguide array. They are easily fabricated and deliver significant amounts of work. A set of bimorph actuators beams, with cross-section and length similar to those of the waveguide beams, is placed on either side of the waveguide beam array. When they are simultaneously powered, the array translates in the out-of-plane direction (*y*). When they are differentially powered, rotation around the light propagation direction (*z*) is achieved. The bimorph effect is obtained by depositing a layer of boron-doped polycrystalline silicon (poly-Si) on top of the SiO_2 beam; the poly-Si structure is both the heater and the structural layer of the actuator.

For in-plane translation (*x*-direction) a chevron actuator is proposed [7]. The actuator beams consist of the same SiO_2 and poly-Si stack. Their expansion upon heating is limited, even for a fairly spacious design. To amplify the chevron motion, a lever mechanism is used.
The combination of SiO_2 and poly-Si (16 µm and 5 µm thick, respectively) has implications for the post-release deformation and actuator behaviour. Both material layers are grown and deposited at high temperature. The difference in CTE (coefficient of thermal expansion) will result in a post-release curvature. For the chevron actuator, this implies that the actuator will have a complex post-release deformation state, with both in-plane and out-of-plane components. Also, when operated, the actuator will have a parasitic out-of-plane motion, next to the desired in-plane motion.
The bimorph actuator beams will also have a post-release

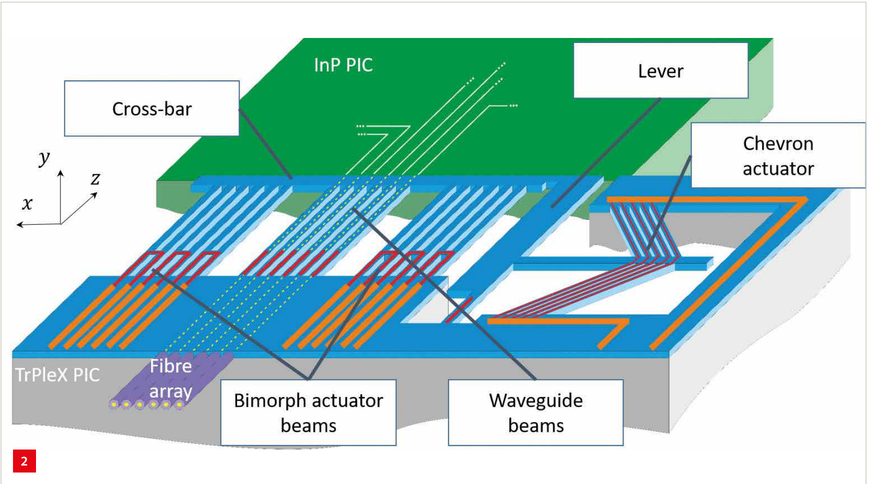

2 *Overview of a typical design. A number of waveguide beams is connected through a cross-bar to sets of bimorph actuators for out-of-plane translation and rotation around the light propagation direction. A chevron actuator, of which the motion is amplified by a lever, generates in-plane motion.*

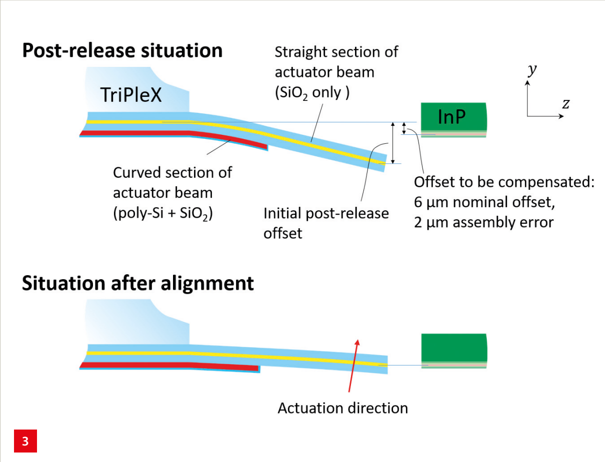

3 *Side view of an actuator beam. Only the initial section of the beam is provided with poly-Si, the length of this section determines the initial post-release offset. An offset of ~8 µm needs to be compensated.*

curvature, and this can be quite significant. The bimorph actuator design proposed makes intended use of the post-release deformation [8]. In this design, only a short section of the entire actuator beam is provided with poly-Si. This section will have a post-release curvature, whereas the remaining SiO_2-only section of the beam is almost straight. Hence, the length of the poly-Si section is a parameter that can be used to fine-tune the initial out-of-plane position of the structure.

This is illustrated in Figure 3, which shows a side view of the spatial relation between the chips' waveguide structures. A nominal offset between the waveguide layers of ~6 µm in the vertical direction exists, due to the definition of the material stacks in the optical layers and in the bond-pads. Also, there will be an error in the vertical direction in the flip-chip bonding process (±1-2 µm, chip-to-chip). Taking this together, the maximum initial offset between the waveguide end-facets that can be expected is ~8 µm. The length of the poly-Si section is chosen to provide this initial offset. When powering the actuator, the optimal position is achieved.

Results

Along the lines of these principles, a wide range of structures was fabricated. Figure 4 shows two examples: to the left, a simple configuration consisting of four bimorph actuator beams, together with a chevron actuator and lever. To the right, a design consisting of six waveguide beams in the centre, and two adjacent sets of bimorph beams.

Motion measurement results are shown in Figure 5, for the chip of Figure 4a. The bimorph actuators consist of 40-µm long poly-Si tracks on 900-µm long SiO_2 beams. The chevron actuator is rigidly connected through the lever mechanism to the cross-bar and actuator beams. Since all structures are connected, mechanical cross-talk can be expected. When only one of the bimorph actuators is powered, the entire structure will deform, i.e. also the end-points of the non-powered beams will move.

For instance, see Figure 5a, when operating the left-side bimorph actuators, i.e. the ones furthest away from the lever and chevron structure, the end-points of the corresponding beams move ~3 µm out-of-plane at 55 mW power. At the same time, the end-points of the other beams are also deflected out-of-plane (~1 µm). Operating the other actuator set shows similar behaviour, see Figure 5b. In this case, the out-of-plane motion is smaller at the same power levels, because of the stiffness of the nearby lever and chevron actuator structure.

Figure 5c shows the results of an in-plane motion measurement for the same chip. The central beam of the chevron actuator moves ~600 nm at ~125 mW, while the cross-bar moves ~1.8 µm; this amplification corresponds to the designed ratio of the lever mechanism. The parasitic out-of-plane motion of the chevron actuator is significant, and was measured to be in the order of a few 100 nm.

To demonstrate the actual coupling of light, a chip with a waveguide array and bimorph actuators on either side of the waveguide array was pre-positioned with respect to an InP PIC using microstages in a laboratory bench set-up. Voltage was applied to the bimorph actuators across the safe operation range (0-55 V) in steps of 1 V. For each combination of actuator voltages the intensity profile for a number of adjacent waveguides at the remote end of the TriPlex chip was measured using an IR camera, which is sensitive to the 1,550 nm wavelength generated by the InP PIC.

Figure 6 shows the intensity profile of one of the waveguides as a function of actuator voltages applied to the left- and right-side actuator, respectively. A maximum in coupled light can be found for different combinations of actuator

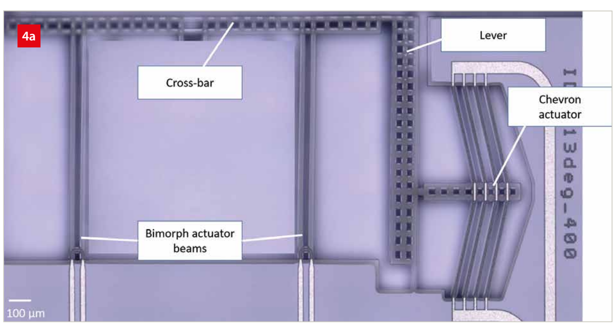

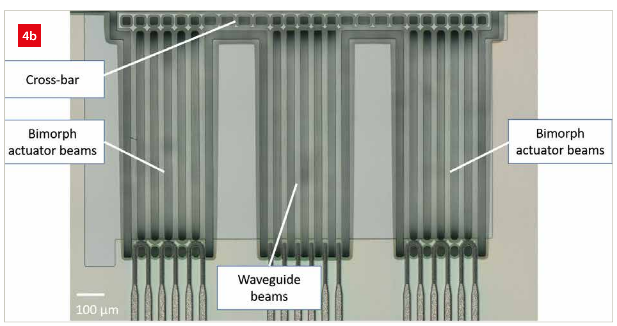

4 *Examples of fabricated devices.*
(a) Configuration consisting of four bimorph actuator beams together with a chevron actuator and lever.
(b) Configuration consisting of six waveguide beams in the centre, and two adjacent sets of bimorph beams.

5 *Motion measurements on the chip of Figure 4a.*
(a) Out-of-plane motion measurement when powering the left-side bimorph actuators.
(b) Out-of-plane motion measurement when powering the right-side bimorph actuators.
(c) In-plane motion measurement when powering the chevron actuator.

6 *Result of an optical coupling experiment, showing normalised light intensity of a single waveguide as a function of combinations of bimorph actuator voltages applied to the left-side (L) and right-side (R) actuator set, respectively.*

7 *PIC with positionable waveguide array and fibre array, bonded to a PCB for testing purposes. (Photo: Hans de Lijser)*

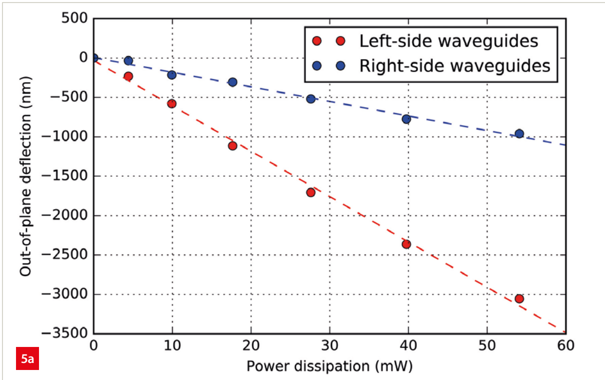

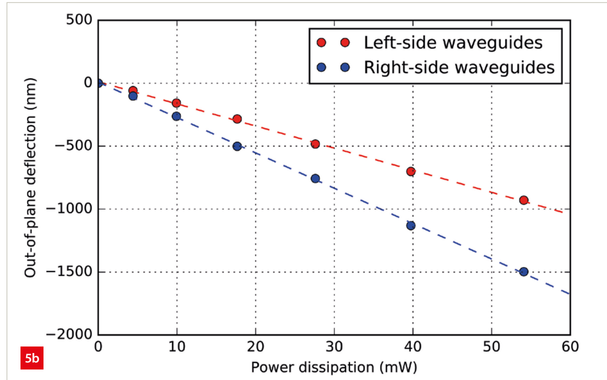

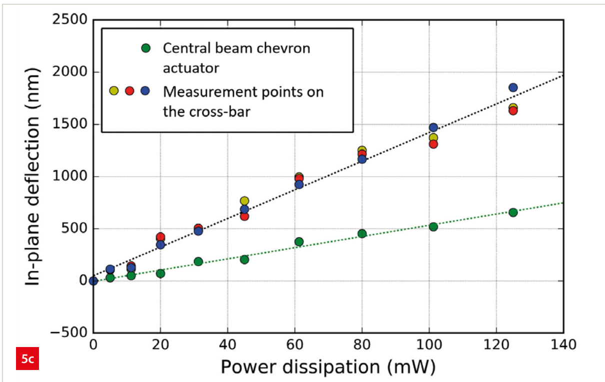

voltages. To place the waveguide array in the globally optimal position, the intensity profiles for the individual waveguides need to be combined [9].

Conclusions and outlook

A concept has been proposed for the automated precision alignment of multi-port photonic chips, combining flip-chip bonding and on-chip alignment of flexible waveguide structures. The principles for chip design and fabrication have been explored, and designs are manufacturable which offer alignment capabilities in the three critical motion directions; Figure 7 shows a tangible result: a PIC with positionable waveguide array and fibre array, bonded to a PCB for testing purposes. Further work will focus on optimising the chip design for performance and size reduction. The main function that needs yet to be developed is the integrated locking.

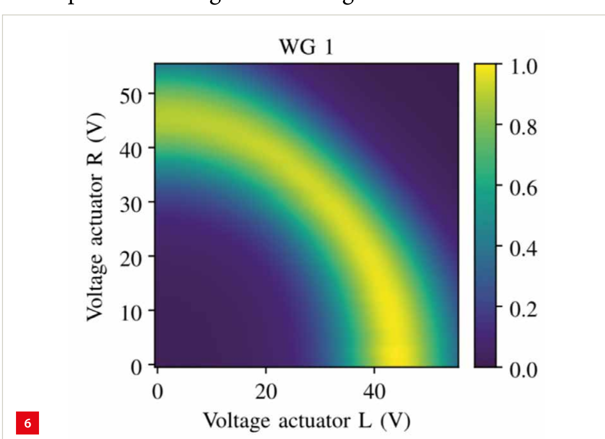

Acknowledgement

Funding for the research leading to these results was received from the STW Generic Technologies for Integrated Photonics (GTIP) programme, grant no. 11355 (Flex-O-Guides), and from the European Community's Seventh Framework Programme FP7/2007-2013 under grant agreement ICT 619267, PHASTFlex. We thank the project partners for their contributions. We specifically thank Tom Scholtes (TU Delft, Else Kooi Laboratory) for microfabrication of the structures in the PHASTFlex project, and Rui Santos (TU Eindhoven) for enabling the optical coupling experiment. ■

REFERENCES

[1] M. Smit et al., "An introduction to InP-based generic integration technology", *Semiconductor Science and Technology* 29, 083001, 2014.
[2] T.J. Peters and M. Tichem, "Mechanically flexible waveguide arrays for optical chip-to-chip coupling", *Proc. SPIE 9760, MOEMS and Miniaturized Systems* XV, 97600D, 2016.
[3] K. Wörhoff et al., "Photonic hybrid assembly through flexible waveguides", *Proc. SPIE 9891, Silicon Photonics and Photonic Integrated Circuits* V, 98911P, 2016.
[4] PHASTFlex FP7 EU Project, *www.phastflex.eu*
[5] K. Wörhoff, R.G. Heideman, A. Leinse and M. Hoekman, "TriPleX: a versatile dielectric photonic platform", *Advanced Optical Technologies* 4, 2015.
[6] T.J. Peters and M. Tichem, "Electrothermal Actuators for SiO_2 Photonic MEMS", *Micromachines* 7, p. 200, 2016.
[7] K. Wu and M. Tichem, "In-plane positioning of flexible silicon-dioxide photonic waveguides", *International Conference on Manipulation, Automation and Robotics at Small Scales (MARSS)*, 2017.
[8] K. Wu and M. Tichem, "Post-release Deformation and Motion Control of Photonic Waveguide Beams by Tuneable Electrothermal Actuators in Thick SiO_2", submitted for publication.
[9] T.J. Peters and M. Tichem, "On-Chip Positionable Waveguides for Submicrometric Photonic Alignment", *Journal of Microelectromechanical Systems* 26, pp. 1259-1271, 2017.